Journal of Pharmaceutical Analysis 7 (2017) 324–331

Contents lists available at ScienceDirect

Journal of Pharmaceutical Analysis

journal homepage: www.elsevier.com/locate/jpa

Original Research Article

Analysis of penicillamine using Cu-modified graphene quantum dots synthesized from uric acid as single precursor

Gema M. Durán[a,b], Tomás E. Benavidez[c], Ana M. Contento[a], Angel Ríos[a,*], Carlos D. García[c,*]

[a] Department of Analytical Chemistry and Food Technology, University of Castilla-La Mancha, Camilo José Cela Av., Ciudad Real E 13004, Spain
[b] IRICA (Regional Institute of Applied Scientific Research), Camilo José Cela Av., E 13004 Ciudad Real, Spain
[c] Department of Chemistry, Clemson University, 219 Hunter Laboratories, Clemson, SC 29634, USA

ARTICLE INFO

Keywords:
Graphene quantum dots
One-step synthesis
Fluorescence quenching
Penicillamine
Pharmaceutical preparations

ABSTRACT

A simple methodology was developed to quantify penicillamine (PA) in pharmaceutical samples, using the selective interaction of the drug with Cu-modified graphene quantum dots (Cu-GQDs). The proposed strategy combines the advantages of carbon dots (over other nanoparticles) with the high affinity of PA for the proposed Cu-GQDs, resulting in a significant and selective quenching effect. Under the optimum conditions for the interaction, a linear response (in the 0.10–7.50 μmol/L PA concentration range) was observed. The highly fluorescent GQDs used were synthesized using uric acid as single precursor and then characterized by high resolution transmission electron microscopy, Raman spectroscopy, X-ray diffraction, Fourier transform infrared spectroscopy, fluorescence, and absorption spectroscopy. The proposed methodology could also be extended to other compounds, further expanding the applicability of GQDs.

1. Introduction

The development and application of nanomaterials is one of the current trends of nanoscience and nanotechnology [1–4]. Among those, photoluminescent nanomaterials have drawn increasing attention because they have the potential to impact a wide number of fields ranging from optoelectronics to bio-analysis [5,6]. While the synthesis and applications of semiconductor quantum dots (S-QDs) [2,7–11] have gained abundant recognition [11], their toxicity can severely impair their use, especially for biomedical applications. Addressing this limitation, carbon-based QDs (CQDs) present themselves as an attractive alternative. Similar to traditional QDs, CQDs exhibit unique optical and electronic characteristics, including large two-photon excitation cross-sections, lack of blinking, high water solubility, biocompatibility, and low toxicity [12–15]. Because these nanomaterials can be synthesized in the 2–20 nm range, they are also intrinsically photoluminescent, a property largely associated to the quantum confinement, their edge structure, and the presence of surface defects [16–22]. Different approaches have been proposed to obtain CQDs, including electrochemical synthesis [23], arc discharge [24], and laser ablation [25]. Most of these top-down approaches involve a non-selective exfoliation process that requires the use of toxic reagents and/or specific facilities. Bottom-up approaches involving the carbonization of various organic precursors (citric acid, glucose, sucrose, glycol, ascorbic acid, etc.) have also been applied to obtain luminescent carbon-based nanomaterials [5,26,27]. However, these approaches typically require several steps to control their water solubility and luminescence properties [25]. An additional limitation affecting both methods is that the resulting particles often contain a significant proportion of amorphous carbon, thus limiting their use. Aiming to address these drawbacks, this study develops a simple, fast and economical approach to producing high quality and photoluminescent graphene quantum dots (GQDs). The GQDs were synthesized via a hydrothermal process using uric acid as a single, low-cost carbon and nitrogen source. To the best of our knowledge, this is the first time that GQDs are synthesized from uric acid as single precursor (with constant C/N ratio). This methodology yields hydrophilic GQDs with competitive photoluminescent properties, and narrow size distribution which can be used for the development of a variety of fluorescent sensing analytical systems.

Among the potential targets with pharmaceutical relevance, penicillamine (PA) is a natural compound containing sulphur amino acids derived from hydrolytic degradation of penicillin-based antibiotics. Its importance relies on its use for the treatment of hepatolenticular degeneration (Wilson´s disease) as well as other disorders (rheumatoid arthritis, primary biliary cirrhosis, scleroderma, fibrotic lung diseases, cystinuria, heavy element poisoning, and progressive systemic sclero-

Peer review under responsibility of Xi'an Jiaotong University.
* Corresponding authors.
E-mail addresses: angel.rios@uclm.es (A. Ríos), cdgarci@clemson.edu (C.D. García).

http://dx.doi.org/10.1016/j.jpha.2017.07.002
Received 16 May 2017; Received in revised form 23 June 2017; Accepted 4 July 2017
Available online 06 July 2017

sis) [28,29]. Due to poor tolerance (abdominal pain, nausea, and diarrhea) and a range of adverse effects, content of PA in pharmaceutical preparations should be closely monitored. Therefore, the development of fast, simple, sensitive, and selective methods for the determination of this analyte is very important from not only the therapeutic but also the regulatory standpoint. Chemically, PA is considered as a strong chelating agent and presents a good reactivity with most heavy metals and forms stable complexes with copper ions [30,31]. Taking this property into account, the present report presents a simple approach to modifying GQDs with copper (II) ions (Cu-GQDs) and using them as a simple fluorescence detection strategy, based on the synergistic quenching effect of Cu-GQDs by PA. The herein proposed strategy also aims at complementing previous reports focused on the use of other nanoparticles towards the analysis of PA [32–37]. The feasibility of the proposed fluorescent sensor for the quantification of PA in pharmaceutical samples was also demonstrated.

2. Materials and methods

2.1. Chemicals and reagents

Uric acid (UA, ≥ 99.0%) was purchased from Alfa Aesar (Ward Hill, MA, USA), and sulfuric acid (ACS/FCC, BDH ARISTAR, 95.0%–98%) was acquired from VWR (Pittsburgh, PA, USA). Sodium hydroxide (98%), copper (II) chloride (99.999%), sodium acetate (≥ 99.0%), acetic acid (≥ 99.7%), and D-penicillamine (PA, ≥ 98%) were obtained from Sigma Aldrich (Germany). All aqueous solutions were prepared using 18.2 MΩ cm water, purified with a Milli-Q water system (Millipore, Molshem, France). Solvents such as methanol (99.9%), absolute ethanol (99.8%), acetone (≥ 99.9%), and acetonitrile were obtained from Panreac (Barcelona, Spain) and chloroform (≥ 99%) was obtained from Sigma Aldrich (Steinheim, Germany). All the reagents were used as received. Acetate buffer solution was prepared by mixing 0.1 mol/L sodium acetate and 0.1 mol/L acetic acid solutions in the proper proportions to get the required pH in the 3.0–6.0 range [38]. $CuCl_2$ modified GQDs (Cu-GQDs) solution was prepared by mixing an appropriate concentration of $CuCl_2{\cdot}H_2O$ solution (0.1 mol/L) and GQDs solution in a 1:19 ratio (m/m). Then the mixture was stirred for 5 min and stored at room temperature in the darkness until use.

Other compounds used in the interference study were sucrose, lactose, glucose, sodium dodecyl sulphate (SDS), starch, sodium chloride, and potassium chloride; all of them were obtained from Sigma (Madrid, Spain).

2.2. Instrumentation

The morphology of the GQDs was determined using a high-resolution transmission electron microscopy (HRTEM) at an accelerating voltage of 200 kV (JEOL 2010-F Field Emission Transmission Electron Microscope). All UV–Vis absorption spectra were recorded using a spectrophotometer (SECOMAM UVI Light XS 2) equipped with a LabPower V3 50 for absorbance data acquisition using 10 mm quartz cuvettes. Fluorescence (FL) spectra were obtained on a fluorescence spectrophotometer (Photon Technology International (PTI) Inc. QuantaMaster 40) equipped with a 75-W continuous xenon arc lamp. An ASOC-10 USB interface FeliXGX software was used for data acquisition. The FL of GQDs samples was observed using a handheld UV lamp (model UVLS-28, 115 V ~ 60 Hz, 0.16 Amp.) with long (365 nm) and short (254 nm) wavelength assembly. FTIR spectra were recorded on an FTIR spectrophotometer (IRAffinity-1, Shimadzu Corporation International Marketing Division, Japan). The pH measurements were achieved in a Crison Basic 20 pH-meter with a combined glass electrode (Barcelona, Spain). The GQDs centrifugation was performed with an ultracentrifuge (Centrofriger BL-II model 7001669, J.P Selecta). X-ray diffraction (XRD) analyses were carried out on an X-ray diffraction spectrometer (XRD Rigaku Ultima IV, Rigaku Americas Corporation, USA) with parallel beam and focused beam, small angle and thin films attachment. Raman spectra were recorded in a Raman spectrometer (BWS415-785S with a probe BAC100-785, BWTek, Inc., USA) using a laser power with an excitation port of 785 nm.

2.3. Synthesis and purification of GQDs

GQDs were synthesized from UA by acidic chemical treatment. In this case, 0.5 g of UA was combined with 1 mL of concentrated sulfuric acid and allowed to react under continuous stirring at 200 °C for 1 h. The brown reaction product was allowed to cool down to room temperature and then neutralized with NaOH (to pH ~ 7) under vigorous stirring. The resulting suspension was treated with a mixture of methanol and acetone (1:4, v/v) and filtered through a 0.45 µm membrane to separate large particles. The subsequent purification steps involved the extraction of GQDs in methanol and acetone (1:4, v/v) and centrifugation at 9000 rpm (to precipitate larger particles and salts). Finally, the yellow product was dried under a N_2 stream and stored at room temperature in the darkness until use.

2.4. Quantum yield (QY) measurements

Fluorescein (dissolved in 0.1 mol/L NaOH, FL QY=92.5%) was chosen as standard. The fluorescence and UV–Vis spectra of fluorescein and obtained GQDs were recorded at different concentrations, respectively. Then FL QY of GQDs in water was calculated according to the following equation (Eq. (1)) [39,40]:

$$QY_s = QY_{st}\left(\frac{K_s}{K_{st}}\right)\left(\frac{\eta_s}{\eta_{st}}\right) \quad (1)$$

where QY_S and QY_{St} represent the quantum yield of the sample and the standard, respectively, K is the slope determined by the fluorescence intensity versus the UV–Vis intensity curves, and η is the refractive index of the solvent. In order to minimize the re-absorption effects, absorption in the 10 mm cuvette was kept below 0.10 at the excitation wavelength.

2.5. Sample preparation and analytical procedure

For the preparation of pharmaceutical samples, 3 capsules of Cupripén® 250 (D-Penicillamine, Laboratorios Rubió, S.A., Barcelona, Spain) were accurately weighed and mixed. A portion of the powder obtained, equivalent to the average weight of a capsule, was dissolved in 500 mL of deionized water. Then, the obtained suspension was filtered through a 0.45 µm filter and the filtrate was used to prepare the working solution of PA for the analysis. The interaction studies were performed by recording the fluorescence spectra of Cu-GQDs, 1:19 ratio, in the absence and in the presence of different concentrations of PA in acetate buffer (5 mmol/L, pH 6.0), after 5 min of reaction at room temperature, and preserved from the light. The fluorescence spectrum was measured at excitation wavelength of 362 nm and collecting the emission between 380 and 640 nm. Both the excitation and the emission slit widths were 2 nm. I_0/I was used as analytical signal, where I_0 and I were the fluorescence intensity at 452 nm of the systems in the absence and in the presence of PA, respectively. When samples were analyzed, PA standard solution was replaced by the pharmaceutical samples prepared as described at the beginning of this section.

3. Results and discussion

3.1. Characterization of GQDs

The GQDs herein reported were synthesized using UA as single precursor and different characterization techniques were used in order

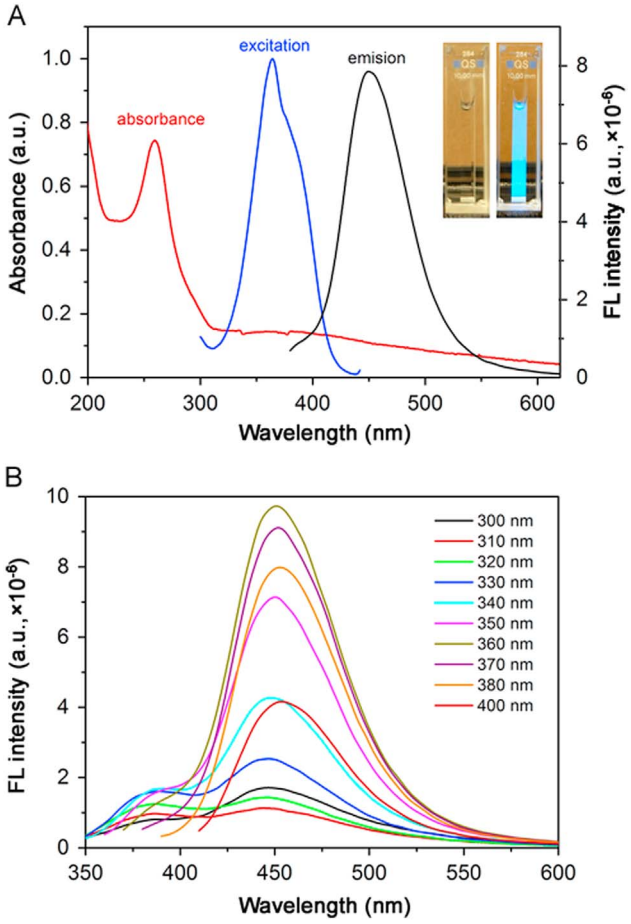

Fig. 1. (A) UV–Vis spectrum (red line), excitation (blue line) and fluorescence spectra (black line) of obtained GQDs, inset: photographs of GQDs solution under visible (left) and 365 nm UV (right) light; (B) fluorescence spectra of GQDs at 300–400 nm excitation wavelengths.

to assess the properties of the GQDs obtained. Optical properties in aqueous media were studied through UV–Vis and FL spectra. As can be observed in Fig. 1A, an absorption peak was observed at 260 nm, typically attributed to π-π* transitions of the aromatic C=C sp^2 domains [41,42]. The broader band (observed at approximately 380 nm) may be attributed to n-π* transitions of C=O bond [43] and the trapping of excited-stage energy by the surface states. The fluorescence spectrum shows a strong emission peak at 452 nm when excited at 362 nm, and the full width at half maximum (FWHM) is about 65 nm, which is similar to the value previously reported for other CQDs [6,16,41,44–46]. In addition, the fluorescence spectrum at different excitation wavelengths shows a maximum intensity at 364 nm. Inserts in Fig. 1A include photographs of the water-dispersed GQDs under either visible or UV light (365 nm). A diluted aqueous GQDs solution shows a faint yellow color, and an intense blue fluorescence color under UV light, which can be easily observed by the naked eye. To further characterize the optical properties of the prepared GQDs, the FL spectra of GQDs were recorded at different excitation wavelengths (Fig. 1B), showing the maximum emission fluorescence at an excitation wavelength of 364 nm. In addition, a slight excitation-dependent fluorescence behavior was observed, shifting to longer wavelengths without a significant change in shape. This fact suggests the presence of abundant surface defects, approximating the trend reported for most of the reported carbon-based nanomaterials. These results also imply that discrete energy levels are present in these nanomaterials [16,41,44,45]. The blue emission was attributed to the free zig-zag effect with a carbine-like triplet ground state of $\sigma^1\pi^1$ [47,48] and their blue luminescence was generated from intrinsic states in the highly crystalline structure. In addition, the effect of increasing concentration of GQDs in aqueous solution on the photoluminiscence intensity was also evaluated. The results showed a linear relationship between photoluminescence intensity and the concentration of nanoparticles in the 0–0.1 mg/mL range.

The absorbance and FL intensity of GQDs at different pH values was also investigated. It was observed that the FL emission intensity of obtained GQDs was pH-dependent, as it was previously reported for this kind of nanoparticles [41,49]. Significant changes in both the FL intensity and the maximum emission wavelength at different pH values were observed (Fig. S1). The FL intensity was increased from pH 2 to pH 6, reaching a maximum value at pH 6. At higher pH values (in the 6–10 range), a blue shift from 452 to 445 nm with decreased FL intensity was observed. This fact can be attributed to the deprotonation of carboxyl groups of G-QDs in alkaline solution, increasing the electrostatic repulsions between them, and overcoming the trend of aggregation through layer-layer stacking [50,51]. This pH-dependent behavior suggests that the origin of photoluminiscence can be linked to small sp^2 fragments conjugated with oxygen-containing functional groups such as carboxylic groups in the GQDs, where the charge and corresponding electronic distribution depend on the pH of the solution [52].

The solubility and fluorescence intensity of GQDs in different solvents was also determined. To this end, powder GQDs was added to several solvents, such as deionized water, glycerol, methanol, ethanol, acetone, acetonitrile, and chloroform. The photographs of GQDs in the several solvents, under visible and 365 nm UV light, demonstrated that solutions of these nanoparticles were stable in deionize water and did not show evidence of sedimentation or agglomeration. While these GQDs can also disperse in other polar organic solvents besides the deionized water, such as glycerol, ethanol, and methanol (Fig. S2), they displayed limited solubility in acetonitrile and acetone and were insoluble in chloroform. Similar to the pH effect, this behavior can be related to the nature of the functional groups of the GQDs. In this context, carbonyl groups in acetone are typical Lewis acid whereas hydroxyl groups in methanol, ethanol, and glycerol are a typical Lewis base [26]. This fact enables to use the obtained GQDs for non-aqueous applications in different fields.

The morphology of prepared GQDs was investigated using HRTEM images, and representative results are shown in Fig. 2A. It can be clearly observed that the produced GQDs consist of small individual particles with a narrow size distribution, ranging between 2.5 and 4.8 nm; with an average value of 3.7 nm (Fig. 2B). This finding suggests that the GQDs consist of dots composed of graphene layers (Fig. 2C), uniformly arranged without apparent aggregation. The HRTEM images also show a lattice fringe of 0.23 nm, in good agreement with the crystal structure of graphene (consistent with the basal plane distance of bulk graphite and the hexagonal lattice) [53]. Moreover, due to their small size, the edge structures such as zig-zag and armchair edges, are more evident based on their HRTEM images, confirming the hexagonal honeycomb structures and bond lengths (1.84 Å of C–C) of graphene (Fig. 2D). These special edges and shapes of the GQDs are responsible for their optical and electronic properties.

The surface and chemical composition of prepared GQDs were determined by FTIR spectra. Fig. 3A shows the FTIR spectra of UA (precursor) and the obtained GQDs. The results reveal the presence of characteristic functional groups in both the precursor and the GQDs. In this way, it was possible to detect the stretching vibration bands of O-H at 3401 cm^{-1}, which indicates the presence of hydroxyl groups and the vibrational absorption band of C–O groups at 1063 cm^{-1}. The presence of the stretching vibration modes of C–H at 3031 cm^{-1} and 1433 cm^{-1}, the vibrational absorption band of C=O conjugated with condensed aromatic carbons at 1671 cm^{-1}, the vibrational absorption band of C–O at 1063 cm^{-1} , and the weak vibration absorption band of N–H at 1595 cm^{-1} were also observed [22,40,54]. It is important to point out that these nitrogen-containing functional groups were considered

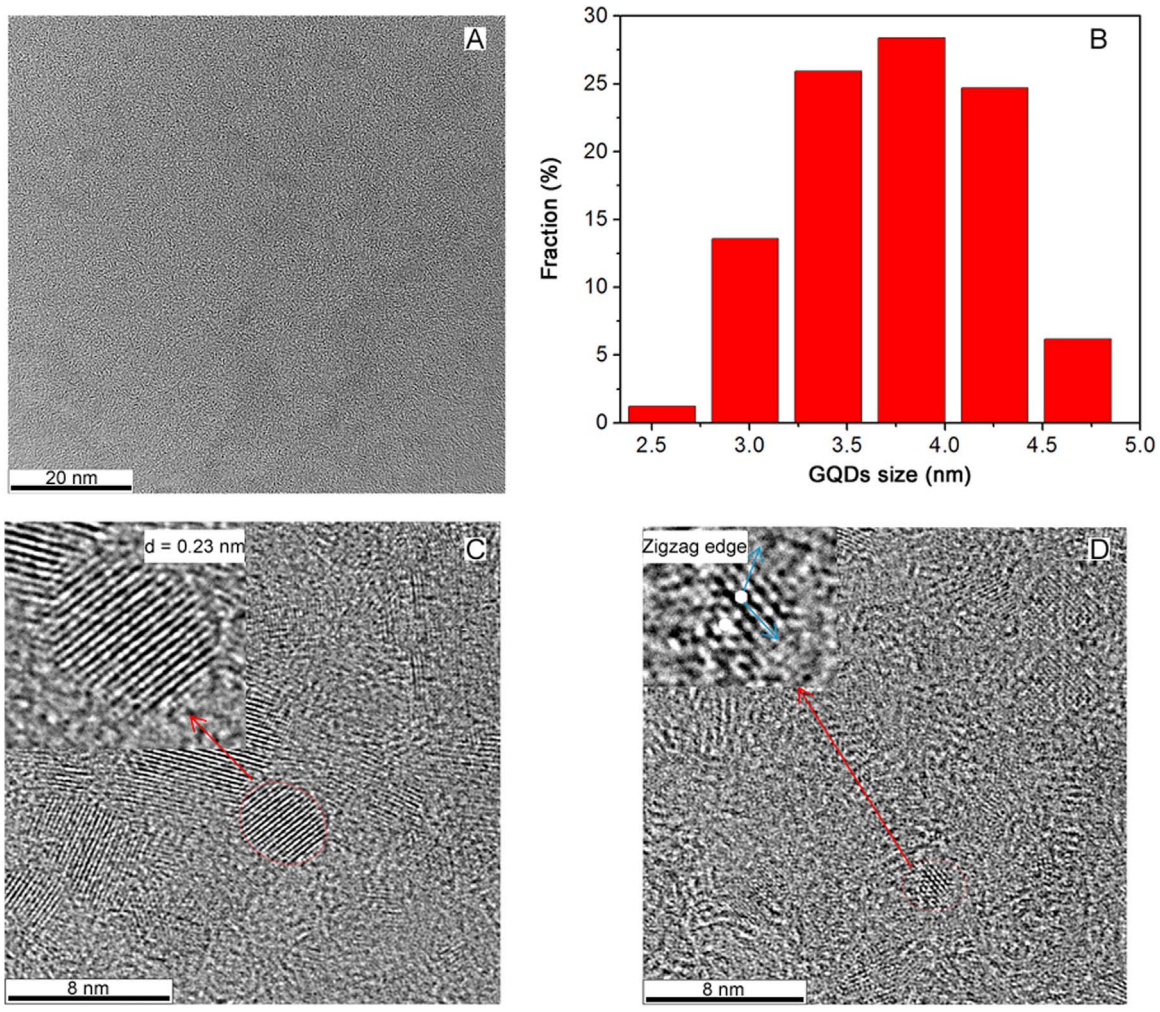

Fig. 2. HRTEM image of (A) GQDs, (B) GQDs size distribution, (C) morphology, and (D) lattice edges (schematic illustration showing the orientation of the graphene and zig-zag edge of a dot).

essential to support the interaction with the copper ions, which would be otherwise released from the surface of the GQDs upon the addition of PA. The XRD pattern in Fig. 3B shows a series of crystalline peaks, forming a broad peak centered at around 29.4° and an interlayer spacing (calculated) of 0.304 nm. This value is broader than that of graphite [55] and it is attributed to the ordered stacking of obtained GQDs.

Raman spectroscopy was used to investigate the structure of the GQDs prepared from UA. Representative results are shown in Fig. 3C, where two characteristic peaks at 1385 cm^{-1} (D band) and 1580 cm^{-1} (G band) were expected. As it can be observed, the D band, resulting from the vibrations of carbon atoms with dangling bonds in the termination plane of carbon structures, clearly dominates the spectrum. It is important to point out that the G band, typically associated with the E_{2g} vibrational mode of aromatic domains in the two-dimensional hexagonal lattice [56], was barely noticeable, an effect that has been associated with the presence of nitrogen atoms [57]. Therefore, considering that graphitic structures were systematically observed by microscopy (Fig. 2A), the ratio of the intensities was used to estimate relative abundance of carbon structures [58]. In our case, a I_D/I_G ratio of 1.35 was calculated for the obtained GQDs, indicating the presence of abundant defects on the obtained GQDs with a partially disordered nanocrystal structure, arising from the small sp^2 cluster size [44].

To further demonstrate the potential advantages of generating GQDs from UA, the quantum yield of these nanoparticles was also calculated, according to the procedure detailed in Section 2.4. In this case, the FL QY of the GQDs resulted to be 44.4%. This value is about 30% higher than that of most conventional GQDs reported in bibliography (Table S1). This enhancement of QY can be attributed to the density of carbene structures in the zig-zag edges, showing interesting luminescence with high quantum yield. Furthermore, compared to other reported GQDs syntheses which involve the use of several precursors, such as citric acid and urea (Table S1), the proposed methodology avoids the amidation reaction due to the use of a single precursor containing a constant (and appropriate) carbon/nitrogen ratio. Therefore, these facts suggest that the optical properties of GQDs are influenced by a combination of factors including their size, shape, and functionalization.

3.2. *Effect of PA on the photoluminescence response of GQDs*

Preliminary interaction studies between the GQDs obtained from UA and PA were carried out by recording the FL spectra of GQDs in the absence and in the presence of PA. It was observed that the presence of PA did not change the FL intensity of GQDs. Thus, it was assumed that PA did not interact with GQDs. However, interesting interactions between synthesized GQDs, previously modified with copper (II) ions (Cu-GQDs), and PA were observed (Fig. S3). It is known that PA is a strong chelating agent presenting good reactivity with copper ions. Thus, the interaction between Cu-GQDs and PA can be studied based on the changes in the FL intensity of modified GQDs. In this regard, the

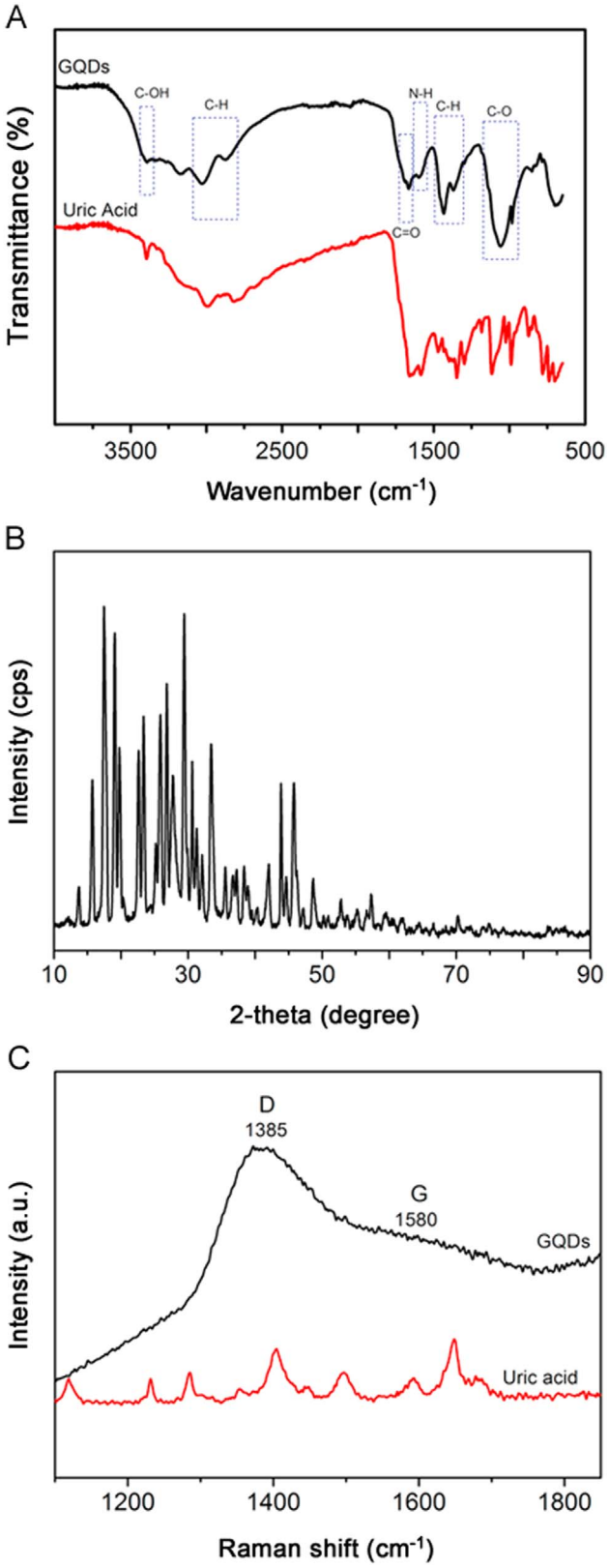

Fig. 3. (A) FTIR spectra of uric acid (red line) and obtained GQDs (black line); (B) XRD patterns of powder GQDs; and (C) Raman spectra of uric acid (red line) and obtained GQDs (black line).

optimization of several chemical variables on the reaction between Cu-GQDs and PA was carried out to obtain the most favorable conditions for the interaction with PA.

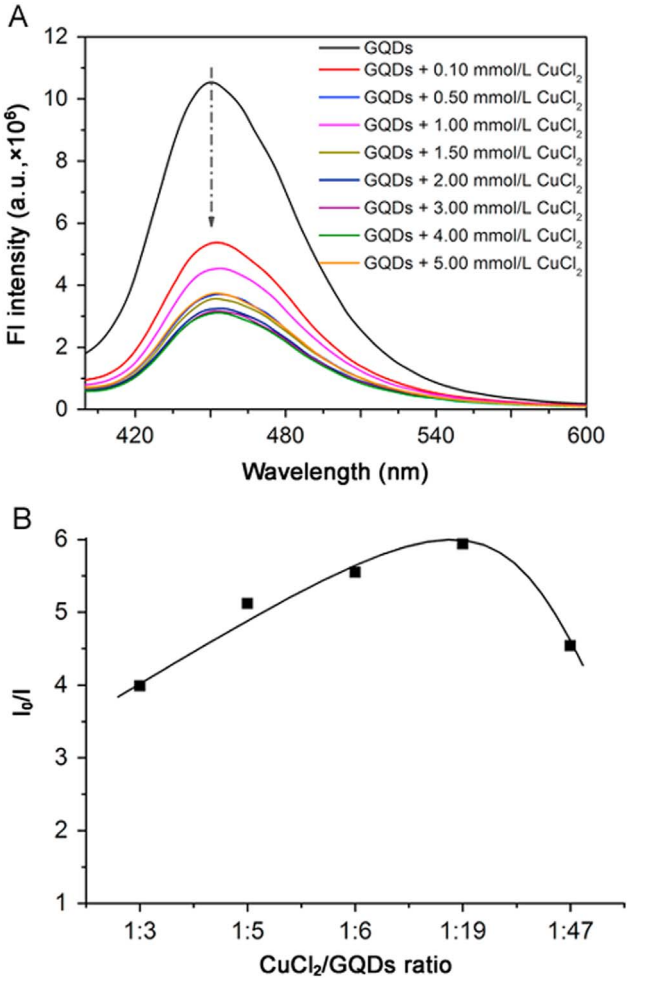

Fig. 4. (A) Effect of increasing concentrations of $CuCl_2$ on the fluorescence intensity of GQDs, and (B) effect of $CuCl_2$/GQDs ratio (C_{PA}=10 μmol/L) in the Cu-GQDs-PA interaction.

In order to evaluate the effect of copper (II) ions on the FL intensity of synthesized GQDs, different concentrations of copper (II) ions between 0.1 and 5.0 mmol/L (13.5–672.3 mg/L) were added to the aqueous solution of GQDs. Then, the FL intensity of the Cu-GQDs system was recorded. It was observed that the FL decreased to about 30% of its initial value when the concentration of copper (II) ions added to GQDs solution was 0.50 mmol/L (Fig. 4A). Higher copper (II) concentration did not produce additional quenching. Therefore, in order to avoid the use of high concentrations of cupric ions, the effect of $CuCl_2$/GQDs ratio in the PA sensing was also investigated. For this purpose, different $CuCl_2$/GQDs ratios in the 1:3 to 1:47 range in the absence (I_0) and in the presence (I) of 10 μmol/L PA were studied (Fig. 4B). A maximum analytical signal was found when the $CuCl_2$/GQDs ratio of 1:19 was used. Therefore, this ratio was selected as optimum and was used for the determination of PA in pharmaceutical preparations.

The selection of the buffer composition was a crucial variable for the reaction. Preliminary studies were conducted using different buffer compositions such as citrate, citrate/phosphate and acetate/acetic acid buffer. A destabilization of the reaction in the presence of citrate and citrate/phosphate buffer was observed, probably due to the reaction with the analyte. However, when acetate/acetic acid buffer was used a stabilization of the system was observed. Therefore, this buffer was used for all subsequent experiments. Moreover, the effect of pH on the FL intensity of the Cu-GQDs system was also evaluated using acetate/acetic buffer ranging from pH 3.0 to 6.0 in the absence (I_0) and in the

presence of 10 μmol/L PA (I). I_0/I was used as the analytical signal. It was found (data not shown) that the pH significantly influenced the FL intensity of the Cu-GQDs-PA system, resulting in a progressive enhancement of I_0/I when the pH was increased and reaching a maximum I_0/I value at pH 6. Therefore, this value was selected as optimum for the subsequent experiments. Additionally, the effect of the buffer concentration of 2–10 mmol/L at pH 6 in Cu-GQDs-PA system was also investigated. No significant differences were found in the I_0/I. However, slight differences in the stabilization time of the system were observed. Specifically, a faster stabilization of the system was observed when the buffer concentration was 5 mmol/L. Higher buffer concentrations led to slower stabilization of the system. Therefore, 5 mmol/L was selected as optimum buffer concentration. On the other hand, studies on the reaction time showed (data not shown) that FL intensity remained constant after stirring the mixture for 30 s and performing the measurements after 5 min of reaction.

FL detection is a useful alternative for the sensitive monitoring of the concentration of PA. Therefore, the analytical use of carbon-based nanomaterials, such as GQDs, can play an important role in the detection of compounds of interest. This fact is due to the presence of sp^2 bonded carbon lattices and surface functional groups, which facilitate the interaction of other moieties to their surface through electrostatic interaction, π–π stacking, and chemical reactions. It is known that metallic ions (such as Hg^{2+}, Fe^{3+} and Cu^{2+}) can bind with carbon-based QDs through surface functional groups or even through surface adsorption quenching the fluorescence of GQDs [59–61]. Moreover, PA can coordinate with metal ions (such as Cu^{2+}) through complexation reaction. Thus, metallic ions may act as a linking agent between GQDs and PA molecules to bring them into proximity of each other, leading to the fluorescence quenching of the Cu-GQDs system. In this context, the Cu-GQDs system can be used as fluorescent probe for the determination of PA.

3.3. Analytical features for the determination of PA

In order to investigate the possible analytical applicability of the obtained GQDs in the presence of copper (II) ions, as fluorescent sensing systems, several analytical performance characteristics were evaluated. PA was used as an analyte under the optimized experimental conditions and the procedure was described in Section 2.5. As it can be observed, with the increase of PA concentration, a progressive decrease in the fluorescence of Cu-GQDs was observed (Fig. 5).

I_0/I was used as a possible analytical signal, where I_0 and I were the fluorescence intensity at 452 nm of the systems (exciting at 364 nm) in the absence and in the presence of PA, respectively. The obtained experimental data were satisfactorily fitted according to a Stern-Volmer plot equation (Eq. (2)), obtaining a good relationship ($r > 0.997$) in the 0.10–7.5 μmol/L range:

$$\frac{I_0}{I} = 1.015 + 0.289[PA] \quad (2)$$

The precision of the methodology was evaluated in terms of repeatability and reproducibility. To determine the repeatability of the methodology, 10 analyses of samples containing 1 μmol/L of PA were carried out and the obtained relative standard deviation (R.S.D.) was 1.51%. Then, the reproducibility was estimated for three replicates of 1 μmol/L PA under inter-day conditions (for two consecutive days), obtaining an R.S.D. of 8.02%. A limit of detection (LOD) of 0.03 μmol/L was obtained for PA determination, based on the IUPAC method (blank signal plus 3 times its standard deviation, n=10)

In order to apply the proposed analytical method to pharmaceutical formulations, a selectivity study was performed considering the usual excipients present in these types of samples. While many studies have reported that the fluorescence of QDs can be affected by metallic cations, it is unlikely that pharmaceutical samples could be contaminated with metallic cations. For this reason, the interference study was performed by adding the possible interfering compounds to a solution containing Cu-GQDs and 1 μmol/L of PA. Possible interfering compounds of pharmaceutical formulations such as magnesium stearate, quinolone, and titanium oxide were eliminated by introducing a previous filtration step of the sample since these compounds are water-insoluble. Moreover, other common excipients such as sucrose, fructose, lactose, glucose, maltose, starch, SDS, K^+, and Na^+ were studied. The results showed that compounds typically present in these samples (in a 1:5 concentration ratio) only provided marginal changes (< 4%) in the analytical signal of Cu-GQDs (Fig. 6). While it is reasonable to expect cross-reactivity with other copper-quelating drugs like tetramines (also used in Wilson's disease [62]), or compounds used in general chelation therapy [63], we do not expect pharmaceutical preparations containing PA to be contaminated with any of these compounds.

3.4. Analytical application

In order to demonstrate the potential applicability of the proposed sensing system for pharmaceutical analysis, the determination of PA in a pharmaceutical sample (Cupripen® 250) was performed. This sample

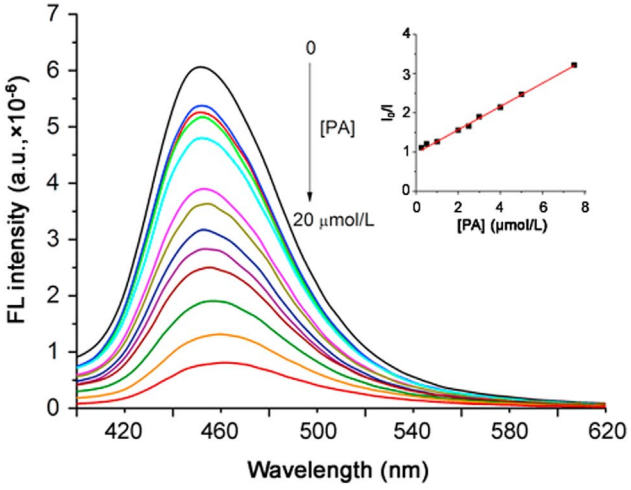

Fig. 5. Fluorescence quenching of Cu-GQDs in the absence and in the presence of different concentrations of PA in the 0.1–20 μmol/L range. Insert: the linear relationship between the relative fluorescence intensity and PA concentration.

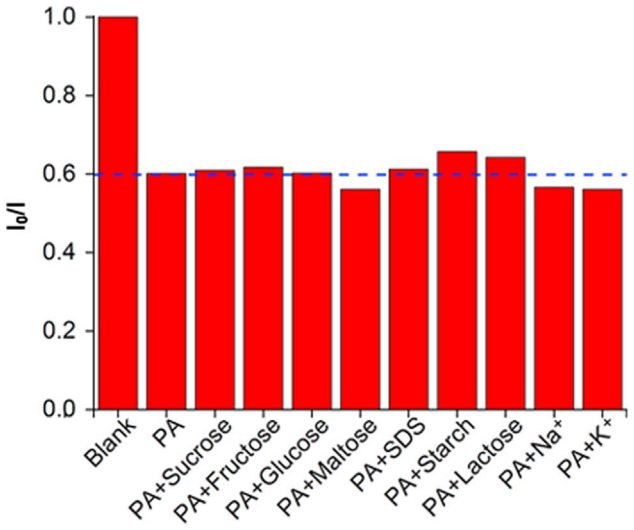

Fig. 6. Relative fluorescence intensity (I/I_0) of Cu-GQDs in the absence and in the presence of 1 μmol/L of PA and 5 μmol/L of different coexisting compounds (sucrose, fructose, glucose, maltose, SDS, starch, lactose, Na^+ and K^+).

Table 1
Determination of PA in pharmaceutical formulation (Cupripen® 250 mg, Laboratorios Rubió, S.A., Barcelona, Spain) by standard addition method (n=3). In all cases, the amount of PA in sample declared by manufacturer was diluted to 0.335 μmol/L.

Amount of standard PA added (μmol/L)	Total PA found (μmol/L)	% Recovery	R.S.D. (%)
0.500	0.88 ± 0.01	112.6	0.8
1.500	1.87 ± 0.02	110.3	1.0
2.000	2.31 ± 0.03	92.3	1.4

was analyzed by triplicate according to the procedure described in Section 2.5. To evaluate the matrix effect, the standard addition method was also used for the determination of PA in the sample and recoveries were examined. The PA content in the real sample was obtained from the standard curve and the regression equation. The results are summarized in Table 1.

As it can be observed, recoveries of PA in the pharmaceutical sample were between 92.3% and 112.6%. The results obtained by the proposed analytical method were compared with the value declared by the manufacturer using the Student statistical t-test. No significant differences were observed.

As such, the developed sensor provides a simple avenue for the determination of PA in different pharmaceutical formulations without the interference of common excipients present in the sample. The analytical performance of the proposed methodology presents clear advantages in terms of simplicity and cost over traditional analytical approaches (like HPLC) or other fluorescent probes based on the interaction of PA with copper ions [64,65]. In addition, the proposed strategy also contributes to complementing previous reports focused on the use of nanomaterials towards the analysis of PA (Table S2).

4. Conclusions

A simple, fast, low-cost, high-yield, and acidic-based treatment method for the synthesis of blue photoluminescence GQDs using a single organic material was developed and the analytical applicability of GQDs was demonstrated. The proposed methodology is suitable for obtaining GQDs with a narrow size distribution (2.5–5.0 nm) which exhibit a characteristic blue luminescence and a competitive quantum yield (44.4%). In addition, the reaction time and the purification process were dramatically shortened, avoiding the longer dialysis purification steps and sophisticated instrumentation (Table S1). Most importantly, the obtained GQDs provide new opportunities for the development of prominent applications due to their high compatibility with aqueous solutions, low cost, and low toxicity. Furthermore, these nitrogen-containing GQDs open facile avenues for the modification with metallic cations and the development of competitive and selective fluorescent probes for the determination of pharmaceutical compounds.

Conflicts of interest

The authors declare that there are no conflicts of interest.

Acknowledgments

This work was partially supported by the NIH–Research Centers at Minority Institutions (G12MD007591), and the projects CTQ2016-78793-P (MINECO of Spain) and PEIC-2014-001-P (Junta de Comunidades de Castilla-La Mancha, JCCM). Gema M. Durán thanks to MINECO of Spain for the predoctoral (BES-2011-045438) and stay (EEBB-I-15-10091) grants.

Appendix A. Supplementary material

Supplementary data associated with this article can be found in the online version at doi:10.1016/j.jpha.2017.07.002.

References

[1] G.M. Durán, T.E. Benavidez, J.G. Giuliani, et al., Synthesis of CuNP-modified carbon electrodes obtained by pyrolysis of paper, Sens. Actuators B 227 (2016) 626–633.
[2] G.M. Durán, T.E. Benavidez, A. Ríos, et al., Quantum dot-modified paper-based assay for glucose screening, Microchim. Acta 183 (2016) 611–616.
[3] E. Evans, E.F. Moreira Gabriel, T.E. Benavidez, et al., Modification of microfluidic paper-based devices with silica nanoparticles, Analyst 139 (2014) 5560–5567.
[4] A.M. Bueno, A.M. Contento, A. Ríos, Validation of a screening method for the rapid control of sulfonamide residues based on electrochemical detection using multi-walled carbon nanotubes-glassy carbon electrodes, Anal. Methods 5 (2013) 6821–6829.
[5] A.B. Bourlinos, A. Stassinopoulos, D. Anglos, et al., Surface functionalized carbogenic quantum dots, Small 4 (2008) 455–458.
[6] H.P. Liu, T. Ye, C.D. Mao, Fluorescent carbon nanoparticles derived from candle soot, Angew. Chem. Int. Ed. 46 (2007) 6473–6475.
[7] G.M. Durán, M.R. Plata, M. Zougagh, et al., Microwave-assisted synthesis of water soluble thiol capped CdSe/ZnS quantum dots and its interaction with sulfonylurea herbicides, J. Colloid Interface Sci. 428 (2014) 235–241.
[8] G.M. Durán, A.M. Contento, A. Ríos, β-cyclodextrin coated CdSe/ZnS quantum dots for vanillin sensoring in food samples, Talanta 131 (2015) 286–291.
[9] G.M. Durán, A.M. Contento, A. Ríos, Use of Cdse/ZnS quantum dots for sensitive detection and quantification of paraquat in water samples, Anal. Chim. Acta 801 (2013) 84–90.
[10] G.M. Durán, A.M. Contento, A. Ríos, A continuous method incorporating β-cyclodextrin modified CdSe/ZnS quantum dots for determination of ascorbic acid, Anal. Methods 7 (2015) 3472–3479.
[11] G.M. Durán, A.M. Contento, A. Ríos, Sensoring strategies using quantum dots: a critical view, Curr. Org. Chem. 19 (2015) 1134–1149.
[12] Y.D. Dong, J.W. Shao, C.Q. Chen, et al., Blue luminescent graphene quantum dots and graphene oxide prepared by tuning the carbonization degree of citric acid, Carbon 50 (2012) 4738–4743.
[13] J. Shen, Y. Zhu, X. Yang, et al., Graphene quantum dots: emergent nanolights for bioimaging, sensors, catalysis and photovoltaic devices, Chem. Commun. 48 (2012) 3686–3699.
[14] S.J. Zhuo, M.W. Shao, S.T. Lee, Upconversion and downconversion fluorescent graphene quantum dots: ultrasonic preparation and photocatalysis, ACS Nano 6 (2012) 1059–1064.
[15] S.T. Yang, L. Cao, P.G. Luo, et al., Carbon dots for optical imaging in vivo, J. Am. Chem. Soc. 131 (2009) 11308–11309.
[16] D.Y. Pan, L. Guo, J.C. Zhang, et al., Cutting sp2 clusters in graphene sheets into colloidal grapheme quantum dots with strong green fluorescence, J. Mater. Chem. 22 (2012) 3314–3318.
[17] F. Xu, H. Shi, X. He, et al., Masking agent-free and hannel-switch-mode simultaneous sensing of Fe^{3+} and Hg^{2+} using dual-excitation graphene quantum dots, Analyst 140 (2015) 3925–3928.
[18] L.A. Ponomarenko, F. Schedin, M.I. Katsnelson, et al., Chaotic dirac billiard in graphene quantum dots, Science 320 (2008) 356–358.
[19] Y.Q. Sun, S.Q. Wang, C. Li, et al., Large scale preparation of graphene quantum dots from graphite with tunable fluorescence properties, Phys. Chem. Chem. Phys. 15 (2013) 9907–9913.
[20] Y. Liu, B. Gao, Z. Qiao, et al., Gram-scale synthesis of graphene quantum dots from single carbon atoms growth via energetic material deflagration, Chem. Mater. 27 (2015) 4319–4327.
[21] S. Zhu, S. Tang, J. Zhang, et al., Control the size and surface chemistry of graphene for the rising fluorescent materials, Chem. Commun. 48 (2012) 4527–4539.
[22] K. Habiba, V.I. Makarov, J. Avalos, et al., Luminescent graphene quantum dots fabricated by pulsed laser synthesis, Carbon 64 (2013) 341–350.
[23] Q.L. Zhao, Z.L. Zhang, B.H. Huang, et al., Facile preparation of low cytotoxicity fluorescent carbon nanocrystals by electrooxidation of graphite, Chem. Commun. (2008) 5116–5118.
[24] X.Y. Xu, R. Ray, Y.L. Gu, et al., Electrophoretic analysis and purification of fluorescent single-walled carbon nanotube fragments, J. Am. Chem. Soc. 126 (2004) 12736–12737.
[25] Y.P. Sun, B. Zhou, Y. Lin, et al., Quantum-sized carbon dots for bright and colorful photoluminescence, J. Am. Chem. Soc. 128 (2006) 7756–7757.
[26] D.Y. Pan, J.C. Zhang, Z. Li, et al., Observation of pH-, solvent-, spin-, and excitation-dependent blue photoluminescence from carbon nanoparticles, Chem. Commun. 46 (2010) 3681–3683.
[27] H.T. Li, X.D. He, Y. Liu, et al., One-step ultrasonic synthesis of water-soluble carbon nanoparticles with excellent photoluminescent properties, Carbon 49 (2011) 605–609.
[28] M. Zeeb, M.R. Ganjali, P. Norouzi, et al., Selective determination of penicillamine by on-line vapor-phase generation combined with Fourier transform infrared spectrometry, Talanta 78 (2009) 584–589.
[29] M.A. Saracino, C. Cannistraci, F. Bugamelli, et al., A novel HPLC-electrochemical detection approach for the determination of d-penicillamine in skin specimens, Talanta 103 (2013) 355–360.

[30] J.R. Wright, Properties of the red-violet complex of copper and penicillamine and further insight into its formation reaction, Bioinorg. Chem. 4 (1975) 163–175.
[31] A. Gergely, I. Sóvágó, Complexes of sulfur-containing ligands. factors influencing complex formation between D-penicillamine and copper(II) ion, Bioinorg. Chem. 9 (1978) 47–60.
[32] T. Naghdi, M. Atashi, H. Golmohammadi, et al., Carbon quantum dots originated from chitin nanofibers as a fluorescent chemoprobe for drug sensing, J. Ind. Eng. Chem. 52 (2017) 162–167.
[33] G.M. Durán, C. Abellán, A.M. Contento, et al., Discrimination of penicillamine enantiomers using β-cyclodextrin modified CdSe/ZnS quantum dots, Microchim. Acta 184 (2017) 815–824.
[34] L.S. Walekar, S.P. Pawar, U.R. Kondekar, et al., Spectroscopic investigation of interaction between carbon quantum dots and D-penicillamine capped gold nanoparticles, J. Fluoresc. 25 (2015) 1085–1093.
[35] S.P. Pawar, A.H. Gore, L.S. Walekar, et al., Turn-on fluorescence probe for selective and sensitive detection of d-penicillamine by CdS quantum dots in aqueous media: application to pharmaceutical formulation, Sens. Actuators B 209 (2015) 911–918.
[36] K. Yang, L.Q. Chen, H.K. Zhao, et al., Construction of CdSe quantum dots "switch" and its application in pharmaceutical analysis, Chin. J. Lumin. 36 (2015) 312–316.
[37] K. Ngamdee, T. Puangmali, T. Tuntulani, et al., Circular dichroism sensor based on cadmium sulfide quantum dots for chiral identification and detection of penicillamine, Anal. Chim. Acta 898 (2015) 93–100.
[38] J. Lambert, T.A. Muir, Practical Chemistry, 3rd. Ed., London Heinemann, London, 1973.
[39] S.J. Zhuo, M. Shao, S.T. Lee, Upconversion and downconversion fluorescent graphene quantum dots: ultrasonic preparation and photocatalysis, ACS Nano 6 (2012) 1059–1064.
[40] Z.H. Wang, J.F. Xia, C.F. Zhou, et al., Synthesis of strongly green-photoluminescent graphene quantum dots for drug carrier, Col. Surf. B: Biointerfaces 112 (2013) 192–196.
[41] D. Pan, J. Zhang, Z. Li, et al., Hydrothermal route for cutting graphene sheets into blue-luminescent graphene quantum dots, Adv. Mater. 22 (2010) 734–738.
[42] Z. Luo, Y. Lu, L.A. Somers, et al., High yield preparation of macroscopic graphene oxide membranes, J. Am. Chem. Soc. 131 (2009) 898–899.
[43] G. Eda, Y.Y. Lin, C. Mattevi, et al., Blue photoluminescence from chemically derived graphene oxide, Adv. Mater. 22 (2010) 505–509.
[44] Y. Li, Y. Hu, Y. Zhao, et al., An electrochemical avenue to green-luminescent graphene quantum dots as potential electron-acceptors for photovoltaics, Adv. Mater. 23 (2011) 776–780.
[45] J. Lu, P.S. Yeo, C.K. Gan, et al., Transforming C60 molecules into graphene quantum dots, Nat. Nanotechnol. 6 (2011) 247–252.
[46] Y.Q. Dong, N. Zhou, X. Lin, et al., Extraction of electrochemiluminescent oxidized carbon quantum dots from activated carbon, Chem. Mater. 2 (2010) 5895–5899.
[47] C.M. Luk, L.B. Tang, W.F. Zhang, et al., Influence of pH on the fluorescence properties of graphene quantum dots using ozonation pre-oxide hydrothermal synthesis, J. Mater. Chem. 22 (2012) 25471–25479.
[48] S. Zhu, J. Zhang, X. Liu, et al., Graphene quantum dots with controllable surface oxidation, tunable fluorescence and up-conversion emission, RSC Adv. 2 (2012) 2717–2720.
[49] J. Shen, Y. Zhu, C. Chen, et al., Facile preparation and upconversion luminescence of graphene quantum dots, Chem. Commun. 47 (2011) 2580–2582.
[50] D. Li, M.B. Müller, S. Gilje, et al., Processable aqueous dispersions of graphene nanosheets, Nat. Nanotechnol. 3 (2008) 101–105.
[51] R. Ye, C. Xiang, J. Lin, et al., Coal as an abundant source of graphene quantum dots, Nat. Commun. 4 (2013) 2943.
[52] N. Fuyuno, D. Kozawa, Y. Miyauchi, et al., Drastic change in photoluminescence properties of graphene quantum dots by chromatographic separation, Adv. Opt. Mater. 2 (2014) 983–989.
[53] L.B. Biedermann, M.L. Bolen, M.A. Capano, et al., Insights into few-layer epitaxial graphene growth on 4H-SiC(0001) substrates from STM studies, Phys. Rev. B: Condens. Matter Mater. Phys. 79 (2009) 125411.
[54] L. Tang, R. Ji, X. Cao, et al., Deep ultraviolet photoluminescence of water-soluble self-passivated graphene quantum dots, ACS Nano 6 (2012) 5102–5110.
[55] M. Zhang, L.L. Bai, W.H. Shang, et al., Facile synthesis of water-soluble, highly fluorescent graphene quantum dots as a robust biological label for stem cells, J. Mater. Chem. 22 (2012) 7461–7467.
[56] S. Lijima, Helical microtubules of graphitic carbon, Nature 354 (1991) 56–58.
[57] J. Gu, M.J. Hu, Q.Q. Guo, et al., High-yield synthesis of graphene quantum dots with strong green photoluminescence, RSC Adv. 4 (2014) 50141–50144.
[58] H. Tetsuka, R. Asahi, A. Nagoya, et al., Optically tunable amino-functionalized graphene quantum dots, Adv. Mater. 24 (2012) 5333–5338.
[59] F. Yan, Y. Zou, M. Wang, et al., Highly photoluminescent carbon dots-based fluorescent chemosensors for sensitive and selective detection of mercury ions and application of imaging in living cells, Sens. Actuators B 192 (2014) 488–495.
[60] C. Han, R. Wang, K. Wang, et al., Highly fluorescent carbon dots as selective and sensitive "on-off-on" probes for iron(III) ion and apoferritin detection and imaging in living cells, Biosens. Bioelectron. 83 (2016) 229–236.
[61] F. Wang, Z. Gu, W. Lei, et al., Graphene quantum dos as a fluorescent sensing platform for highly efficient detection of copper(II) ions, Sens. Actuators B 190 (2014) 516–522.
[62] M. Patil, K. Sheth, A. Krishnamurthy, et al., A review and current perspective on Wilson disease, J. Clin. Exp. Hepatol. 3 (2013) 321–336.
[63] S. Flora, V. Pachauri, Chelation in metal intoxication, Int. J. Environ. Res. Public Health 7 (2010) 2745–2788.
[64] P. Wang, B. Li, N. Li, et al., A fluorescence detection of d-penicillamine based on Cu^{2+}-induced fluorescence quenching system of protein-stabilized gold nanoclusters, Spectrochim. Acta A Mol. Biomol. Spectrosc. 135 (2015) 198–202.
[65] Y. Zhaib, H. Zhuanga, M. Peia, et al., The development of a conjugated polyelectrolytes derivative based fluorescence switch and its application in penicillamine detection, J. Mol. Liq. 202 (2015) 153–157.